THE EFFECTS OF ELLIPTIC AND RECTANGULAR CUTOUTS ON THE BUCKLING OF CYLINDRICAL SHELLS LOADED BY AXIAL COMPRESSION

Thesis by

Susumu Toda

In Partial Fulfillment of the Requirements

For the Degree of

Aeronautical Engineer

California Institute of Technology

Pasadena, California

1975

(Submitted August 13, 1974)

ACKNOWLEDGMENT

The author wishes to express his great appreciation to Professor E. E. Sechler for his suggesting this problem, his kind and valuable guidance throughout this investigation and his patiently correcting the manuscript. The advice and useful comments of Professors C. D. Babcock and G. W. Housner are also appreciated.

The author would also like to thank Mrs. Fox for patiently typing the manuscript, Mrs. Wood for preparing the figures, and Mr. M. Wood for his kind assistance.

The financial aid provided by The California Institute of Technology and the Sloan Foundation is gratefully acknowledged.

ABSTRACT

The results of experimental investigations of the effect of elliptic cutouts on the buckling of thin cylindrical shells under axial compression are presented. The experiments were performed on Mylar shells with a radius to thickness ratio of 400 and with two diametrically opposed circular, elliptic or rectangular holes. The results show that, for a given shell geometry, the area of a cutout determined the shell buckling behavior, but that the configuration of the cutout had little influence on the buckling loads.

A simplified analytical study based on Van Dyke's stress analysis and a strictly empirical design formula which gives a lower bound for the existing experimental data are also presented.

TABLE OF CONTENTS

LIST OF TABLES

LIST OF FIGURES

NOMENCLATURE

A	Area of the cutout
a	Radius of a circular cutout or Length of major semiaxis of an elliptic cutout
b	Length of minor semiaxis of an elliptic cutout
d	$\pi R/n$
E	Young's modulus
n	Number of cutouts
P	Applied axial load
P_{CL}	Classical buckling load
P_{TOT}	Total load carried at the shell center section
R	Shell radius
r	Distance from hole center
t	Shell thickness
y	Distance from shell axis to applied load
α	$(A/\pi Rt)^{\frac{1}{2}}$
β	$[12(1-\nu^2)]^{\frac{1}{4}} (\frac{a^2}{8Rt})^{\frac{1}{2}}$
μ	$(a+b)/2(Rt)^{\frac{1}{2}}$
η	An empirical factor in Eqn. (9)
σ	Axial compressive stress at shell center cross section
σ_{max}	Maximum value of σ
σ_{∞}	Uniform compressive stress at shell ends
ν	Poisson's ratio

I. INTRODUCTION

In the design of aerospace structures, the effect of cutouts on stress distribution and buckling loads is one of the problems of considerable importance. The interstage section and payload fairings of a three-stage Thor-Delta rocket, for instance, have cutouts that affect the stress distribution and buckling stability (Ref. 1).

The first attempt on the problem of prebuckling stress distribution was made by Lur'e in 1947 (Ref. 2). He obtained a perturbation solution for the stress concentration around a circular hole in the cylinder loaded by axial tension and internal pressure. Later, the extension of Lure's analysis was reported by several authors, for example, by Lekkerkerker (Ref. 3), Van Dyke (Ref. 4) and Savin (Ref. 5). It was shown in these reports that the parameter

$$\alpha = \frac{a}{\sqrt{Rt}}$$

governs the solution of the prebuckling stress distribution and displacements for a circular cylinder with a circular cutout.

Because of the presence of prebuckling bending deformation near a cutout region, the buckling analysis of a circular cylindrical shell with cutouts becomes an essentially nonlinear problem. Tennyson (Ref. 6) reported the results of the experimental investigation of the effect of a single circular cutout on the buckling of axially compressed cylindrical shells with shell radius to thickness ratio ranging from 162 to 331. Jenkins (Ref. 7) performed buckling experiments on cylinders in the parametric range $75 \leq R/t \leq 150$ with two diametrically opposed circular cutouts. Starnes (Ref. 8)

carried out an extensive experimental investigation for the buckling of axially compressed cylinders with one circular cutout. The shell radius to thickness ratio R/t in his experiments ranged from 400 to 960, and the cutout hole radius to shell radius ratio a/R ranged from 0 to 0.5. Based on the experience gained from the experiments, he linearized the problem and obtained an upper bound buckling load by the Rayleigh-Ritz method. Starnes concluded in his report that the parameter α also determines the shell buckling behavior.

The results of a nonlinear collapse analysis for axially compressed cylindrical shells with two diametrically opposed square cutouts was first presented by Brogan and Almroth in 1970 (Ref. 10). Almroth and Holmes (Ref. 11) presented the results of additional numerical analyses and experiments on cylinders with two rectangular cutouts. Almroth, Brogan and Marlowe (Ref. 12) carried out a highly sophisticated nonlinear collapse analysis for axially compressed circular cylindrical shells with two diametrically opposed circular cutouts, and they showed that theoretical results are in good agreement with experimental results provided by Starnes. They also pointed out that virtually the same critical load is obtained whether the cutout is circular or square. Recently Starnes (Ref. 9) presented the results of additional experiments which show the effects of circular, square and rectangular cutouts on the buckling load of a cylinder under axial compression, together with numerical results obtained by the NASTRAN finite element computer program.

Cutout configurations considered in the previous investigation are limited to circle, square and rectangle. In the present research

the effects of elliptic and rectangular cutouts on the buckling of a thin cylindrical shell loaded by axial compression were examined experimentally. Tests were performed on Mylar shells with a radius of 4.0 inches, a thickness of 0.01 inch and a length of 10.5 inches. A series of two diametrically opposed elliptic holes with increasing cutout areas were cut into the shell wall at midlength. Ellipses, which had major axis to minor axis length ratios of 1.0, 1.5 and 2.0, were oriented with their major axes either in the shell axial or circumferential direction according to a given cutout program for each shell. Tests on cylinders with circular and rectangular cutouts were also done for the purpose of comparison. Test results were compared with both those of Starnes and the theoretical analysis by Almroth, Brogan and Marlowe. All of the results in the present experiments fell within the scatter band of experimental results on cylinders with one circular cutout obtained by Starnes. It was shown that shapes of cutouts with constant area have no noticeable effect on the buckling loads and that the parameter

$$\alpha = \left(\frac{A}{\pi R t}\right)^{\frac{1}{2}}$$

governs the shell buckling behavior.

II. EXPERIMENTAL SPECIMENS AND PROCEDURES

2.1 Fabrication of the Test Specimens

The ten cylinders were made from DuPont's Mylar polyester film. A Mylar shell could be buckled many times without permanent damage occurring, so long as excessive postbuckling deformations were prevented. It was possible, therefore, to test the same shell for a series of increasingly larger cutouts and to determine the effect of both cutout size and configuration on the buckling of each cylinder. Details of the advantages and disadvantages of using Mylar as shell buckling specimens were discussed by Babcock in Ref. 13. The Young's modulus and Poisson's ratio were assumed to be equal to 7.25×10^5 psi and 0.3 respectively (Ref. 8).

Sheets of the appropriate size were cut from an available roll stock with nominal thickness of 0.010 inch. A measurement of thickness at 30 points showed this value to be accurate within ±2.0%. Rectangles corresponding to developed cylinders with 0.5 inch wide lap joint seams were drawn on these sheets. Next, reference marks were drawn on the rectangles to locate the cutout centers at the cylinder midlength and at 90° with respect to the lap joint seam center line. Then the sheet was cut to the required rectangle by a large paper cutter, and both ends to be joined were roughened with fine emery paper. The rectangle was attached to an 8-inch diameter wooden mandrel, and Teledyne Pro-Seal 501/501A Mylar adhesive was applied to the prepared lap joint. The cylinder was left on the mandrel for 24 hours with an aluminum bar clamped along the seam. Waxed paper was used to keep the mandrel and the bar from sticking

to the cylinder. After detaching from the mandrel, the cylinder was left for an additional two weeks for complete curing of the seam. An aluminum end plate with a circular groove was attached to each end of a cylinder by fitting the cylinder in the groove filled with Cerrolow, a low melting temperature (110° F) alloy. The top plate had small holes along one of its diameters, at the plate center and at 0.125 inch intervals on either side of the center. The top plate was attached to a cylinder so that the line of small holes would be in the plane of symmetry which also contained the center line of the seam. Ten staples were fixed around the circumference of the cylinder at each end of the shell to prevent the cylinder from pulling out of the Cerrolow during buckling. The resulting Mylar cylinders were 8 inches in diameter, 0.01 inch in thickness and 10 inches long.

2.2 Test Equipment and Procedure

The setup for the tests is shown in Fig. 1. The shell was positioned on the lower table of the testing machine so that the center of the top end plate was directly under the center of the loading screw. The hemispherical cup with a ball bearing was then placed on the top end plate by inserting a short pin on the cup bottom into the center hole of the top end plate. Next the load cell was installed between a ball bearing recessed in the bottom end of the loading screw and the ball bearing in the hemispherical cup. The load cell was calibrated in a 3000-pound Riehle Brothers testing machine, and its spring constant was found to be 2.5 pounds per 0.001 inch deflection of the load cell dial gage. The load was applied as slowly as possible by turning the hand lever fixed on the top end of the loading

screw.

In view of the sensitivity of axially compressed cylindrical shells to initial imperfections, each shell was first tested without any hole in order to provide a reference buckling load. A series of elliptic, circular, or rectangular cutouts with increasing areas were then made on the shell at the midlength and 180° apart on the circumference. Elliptic cutouts were oriented with their major axes vertical in the first series of experiments, and horizontal in the second series. In the third series of experiments, vertical or horizontal ellipses were cut alternately with its size increasing each time. The ratios of the length of major axis to that of minor axis of these ellipses throughout the experiments were fixed to be 1.0, 1.5 and 2.0. In the circular cutout series the circle diameters were determined to give the same cutout areas as the elliptic cutouts. The rectangular cutouts with aspect ratios equal to values of a/b of the ellipses were oriented with their long sides in the shell axial direction.

The cutouts were made by the following procedure. First, the cutout configurations together with their main axes were drawn on Avery self-adhesive labels. The ellipses were drawn using an "ellipsograph." The labels were then pasted on the desired position of the shell wall previously marked. A high-speed Dremel hand drill with various cutting tools and grindstones was used to cut the holes on the shell walls. Any excess material along the hole edges was trimmed off with a sharp blade and then the hole edges were finished with fine emery paper.

The shell was then loaded through the center of the top end plate until it buckled. At buckling there was an audible snap and a sudden decrease in the load indicated by the dial gage in the load cell. This procedure continued until the largest desired hole (a = 2.4 inches, b = 1.6 inches) was made on the cylinder and the corresponding buckling load was measured.

III. RESULTS OF THE EXPERIMENTS

3.1 Experimental Results

The experimental results are summarized in Fig. 2, which shows the normalized buckling loads as a function of the parameter

$$\mu = \frac{a+b}{2\sqrt{Rt}}$$

where R is the shell radius, t is the shell thickness, and a and b are the lengths of the major and minor semiaxes of the cutouts. The measured buckling loads have been normalized by the classical buckling load for a cylinder without a hole given by

$$P_{CL} = \frac{2\pi Et^2}{\sqrt{3(1-\nu^2)}}$$

where E is Young's modulus, and ν is Poisson's ratio. The dashed curves in Fig. 2 represent the upper and lower boundaries of the experimental results for cylinders with a circular cutout presented by Starnes in Ref. 8. Similar results for the individual shell are shown in Figs. 3 through 8 and also presented in Tables 1 through 6. It is seen that almost all the results for the various shaped cutouts in the present experiments fall within the scatter band of the experimental data for cylinders with one circular cutout. The results for the cylinder with vertical rectangular cutouts, which have already been shown in Table 6, and Figs. 2 and 8, are again plotted in Fig. 9 in comparison with Starnes' test results for cylinders with vertical or horizontal rectangular cutouts from Ref. 9. The theoretical results for cylinders with circular or square cutouts reported by Almroth et al.

in Ref. 12 are also shown in Fig. 9.

So far, all the experimental results have been plotted as a function of the parameter μ. Let us now consider the correlation parameter. It was pointed out by Starnes (Ref. 8) that the buckling behavior of the shell with a circular cutout was governed by the parameter

$$\alpha = \frac{a}{\sqrt{Rt}}$$

where a is the hole radius, R is the shell radius, and t is the shell thickness. For the elliptic, or rectangular cutouts, what values could be used in place of the radius of the circle? Taking the characteristic hole dimension to be equal to the average of the lengths of major and minor semiaxes of the cutout, we can first define the parameter μ. Next, after rewriting the parameter α in the form as

$$\alpha = \frac{a}{\sqrt{Rt}} = \sqrt{\frac{\pi a^2}{\pi Rt}} = \sqrt{\frac{A}{\pi Rt}}$$

where A is the cutout area,

we can use also the parameter α as a governing parameter. In the case of circular cutouts, it is obvious that α is equal to μ. Both parameters together with the experimental data for each cylinder are indicated in Tables 1 through 6. Fig. 10, which is a counterpart of Fig. 2, presents a plot of the experimental results against the parameter α. The scatter band of Starnes' experimental results for cylinders with one circular cutout is also plotted for comparison. Fig. 11 shows the effects of elliptic cutouts on the buckling of cylinders.

The dashed curve in Fig. 11 represents the results of a theoretical analysis from Ref. 12.

Experimental results show that the parameter α governs the shell buckling behavior, but the cutout configurations considered within the present report have no significant effects on the buckling loads. For values of α less than 0.5, there was no appreciable effect of the cutouts on the buckling loads, and the shells buckled into the diamond pattern. In this range of α, the stress concentration due to the cutout may not be large enough to cause buckling before the shell buckles into the diamond pattern due to other initial imperfections.

For values of α between 0.5 and 2.0, the buckling loads dropped sharply as α increased. This may imply that the effect of the stress concentration at the edge of the cutout becomes important in this range of α.

For values of α greater than 2.0, the shells always buckled into a stable local buckling mode near the edge of the cutout. After local buckling, the shells still went on to carry additional load until they finally buckled into the general collapse. The buckling loads continued to decrease slowly as α was increased.

Shell No. 5 with a series of horizontal elliptic cutouts was tested under eccentrically applied axial compression. The results are summarized in Table 7 and Fig. 12. In Fig. 12 the normalized buckling loads are plotted with respect to the ratio of the loading eccentricity "y" to the shell radius "R", where y is measured from the center of the top end plate with its positive direction defined

toward the seam. It is seen that, for the values of α equal to 0 and 0.5, the small loading eccentricity has an apparent effect on the buckling loads, but has much less effect for the values of α greater than 0.5. This implies that the initial imperfections are very important in the range of α less than 0.5, while, for values of α greater than 0.5, the stress concentration at the edge of the cutout becomes more important than the initial imperfections.

Fig. 13 and Fig. 14 show the typical general collapse modes for $\alpha < 2$ and $\alpha \geq 2$ respectively.

3.2 Analytical and Empirical Analysis

Let us look at the developed cylinder with two cutouts as shown in Fig. 15. At the upper and lower edges it is loaded with the uniform compressive stress σ_∞. Treating this as a flat plate, the stress distribution along the centerline (through the center of the cutouts) is given by the equation (for example, Ref. 14)

$$\frac{\sigma}{\sigma_\infty} = \frac{1}{2}\left(2 + \frac{a^2}{r^2} + 3\frac{a^4}{r^4}\right) \qquad (1)$$

where a is the hole radius and r is the distance from the center of the hole. This shows a maximum value of $\sigma/\sigma_\infty = 3$ at $r = a$ (edge of the hole) and the value of σ/σ_∞ drops to 1.022 at $r/a = 5$.

For the flat plate, the value of σ_{max} is not a function of the size of the hole. However, as shown by other authors, the value of σ_{max} for a hole in a circular cylinder is dependent upon the hole size and cylinder geometry. Using the results of Van Dyke's analysis for the sufficiently large hole

$$\frac{\sigma_{max}}{\sigma_{\infty}} = 3.05\beta^{\frac{2}{3}} + 1 \qquad (2)$$

where $\beta^2 = \frac{a^2[12(1-\nu^2)]^{\frac{1}{2}}}{8Rt} = 0.413\frac{a^2}{Rt}$

or in the notation of this report

$\beta^2 = 0.413\alpha^2$ for the circular cutout.

Therefore

$$\frac{\sigma_{max}}{\sigma_{\infty}} = 2.27\alpha^{\frac{2}{3}} + 1 \qquad (3)$$

Referring back to Fig. 15, the total load carried across the center section of the shell will be given by

$$P_{TOT} = 2n\int_a^d \sigma t dr \qquad (4)$$

where n is the number of holes and d is given by $\frac{\pi R}{n}$, which is equal to one-half the distance between hole centerlines.

It could be assumed that buckling will take place when the value of σ_{max} is equal to the classical buckling stress σ_{CL} of the cylinder without a hole. However, the stress redistribution around the hole may alter this value and we will therefore assume that buckling will occur when $\sigma_{max} = \eta\sigma_{CL}$ where η will be determined by experiment.

Since the Van Dyke analysis does not give σ as a function of r/a in a suitable form, a distribution will be assumed that will closely match that shown for $\beta = 2$ in Fig. 6 of Ref. 4. The stress

at any value of r/a is assumed to be

$$\sigma = \sigma_{max} - (\sigma_{max}-\sigma_{\infty}) \left(1 + \frac{1}{5}\frac{a^2}{r^2} - \frac{6}{5}\frac{a^4}{r^4}\right) \tag{5}$$

where σ_{max} is the Van Dyke value of

$$\sigma_{max} = (2.27\,a^{\frac{2}{3}} + 1)\,\sigma_{\infty}$$

This leads to

$$\sigma = \sigma_{\infty}\left[1 - 0.454\,a^{\frac{2}{3}}\left(\frac{a^2}{r^2} - 6\,\frac{a^4}{r^4}\right)\right] \tag{6}$$

Substituting (6) for σ in (4) and integrating we get

$$P_{TOT} = 2nt\sigma_{\infty}d\left[1 + \frac{a}{d}\left(0.454\,a^{\frac{2}{3}}-1\right) + 0.454\,a^{\frac{2}{3}}\left(\frac{a^2}{d^2} - 2\,\frac{a^4}{d^4}\right)\right] \tag{7}$$

The load that can be carried by the shell without cutouts is

$$P_{CL} = 2\pi Rt\sigma_{CL} \tag{8}$$

and, from the above discussion

$$\sigma_{max} = \eta\,\sigma_{CL} = \sigma_{\infty}\,(2.27\,a^{\frac{2}{3}} + 1) \tag{9}$$

Therefore

$$\sigma_{\infty} = \frac{\eta\sigma_{CL}}{(2.27a^{\frac{2}{3}} + 1)} \tag{10}$$

Hence, from (7), (8) and (10)

$$\frac{P}{P_{CL}} = \frac{\eta}{2.27\alpha^{\frac{2}{3}}+1}\left[1 + \frac{a}{d}(0.454\alpha^{\frac{2}{3}}-1)+0.454\alpha^{\frac{2}{3}}(\frac{a^2}{d^2} -2\frac{a^4}{d^4})\right] \quad (11)$$

But, since

$$\alpha = \sqrt{\frac{A}{\pi Rt}} = \sqrt{\frac{\pi a^2}{\pi Rt}} = \frac{a}{\sqrt{Rt}}$$

and $d = \frac{\pi R}{2}$ for n = 2,

$$\frac{a}{d} = \frac{2}{\pi}\sqrt{\frac{t}{R}}\,\alpha = 0.03183\alpha$$

$$\frac{a^2}{d^2} = \frac{4}{\pi^2}\,\frac{t}{R}\,a^2 = 1.01321 \times 10^{-3}\,a^2$$

$$\frac{a^4}{d^4} = \frac{16}{\pi^4}\,\frac{t^2}{R^2}\,a^4 = 1.02660 \times 10^{-6}\,a^4$$

for t = 0.01 and R = 4.0.

Therefore, for the test specimens in this program, (11) becomes

$$\frac{P}{P_{CL}} = \frac{\eta}{2.27\alpha^{\frac{2}{3}}+1}\left[1-0.03183\,a + 0.01445a^{5/3}+0.460\times10^{-3}\,a^{8/3} -0.9322 \times 10^{-6}\,a^{14/3}\right] \quad (12)$$

This is plotted in Fig. 16 for $\eta = 1$ and $\eta = 1.4$ in comparison with the scatter band of the experimental data.

It would appear from this very cursory study that, if one could determine the exact stress distribution from the edge of the cutout into the main body of the shell, the above method would lead to agreement between theory and experiment. This distribution probably has four distinct regions, namely,

1) $0 \leq \alpha \leq 0.5$ where initial imperfections are very important,

2) $0.5 \leq \alpha \leq 2$ where the effects of the stress concentration at the edge of the cutout becomes important,

3) $2 \leq \alpha \leq 7$ where the full effect of the cutout has been established, and

4) $\alpha > 7$ or 8 where initial buckling near the edge of the cutout leads to a redistribution of stress and probably large local deformations.

Furthermore, one should consider the fact that bending stresses will also occur in the shell with cutouts, although in the shell without cutouts and in the plate with or without cutouts only membrane stresses are present. Details of the above arguments must be left to other investigators.

As an aid to the designer, a strictly empirical equation has been established which gives a lower bound to the existing experimental values. This is

$$\frac{P}{P_{CL}} = \left(\frac{P}{P_{CL}}\right)_o \left(e^{-\sqrt{\frac{\alpha}{3}}} + 0.01\alpha\right) \tag{13}$$

where $\left(\frac{P}{P_{CL}}\right)_o$ is the average of the experimental values obtained for cylinders without cutouts. For the curves shown, the value of $\left(\frac{P}{P_{CL}}\right)_o$ has been taken as 0.65 and the plot of equation (13) is shown in Fig. 17 in relation to the scatter band curves of the experimental data.

IV. CONCLUSIONS

Within the geometry studied in this report, the effect of the various cutout configurations on the buckling loads of a cylinder is rather small. For a given cutout area, virtually the same buckling loads are obtained whatever the cutout configuration may be. If a cutout is small enough, the stress concentration at the edge of the cutout is not sufficient to cause buckling before the shell buckles due to general initial imperfections. However, larger cutouts result in reduction of the buckling strength of the cylinder. The amount of reduction of the buckling loads depends upon a parameter α which is equal to the square root of the ratio of the area of one cutout to one-half the shell cross-sectional area.

The very simplified approximation based on the Van Dyke prebuckling stress analysis provides a fairly good prediction to the buckling loads. The strictly empirical formula

$$\frac{P}{P_{CL}} = \left(\frac{P}{P_{CL}}\right)_o \left(e^{-\sqrt{\frac{\alpha}{3}}} + 0.01\alpha\right)$$

gives the lower bound for the existing experimental data.

The problem is of considerable practical interest, and deserves further investigations for wider ranges of cutout geometries.

REFERENCES

1. Babel, H. W., Christensen, R. H. and Dixon, H. H., "Design, Fracture Control, Fabrication, and Testing of Pressurized Space-Vehicle Structures," Thin-Shell Structures, edited by Fung, Y. C. and Sechler, E. E., Prentice Hall, 1974, pp. 549-600.

2. Lur'e, A. I., Statics of Thin-Walled Elastic Shells, State Publishing House of Technical and Theoretical Literature, Moscow, 1947; Translation, AEC-tr-3798, 1959, Atomic Energy Commission.

3. Lekkerkerker, J. G., "On the Stress Distribution in Cylindrical Shells Weakened by a Circular Hole," Ph.D. Thesis, Technological University, Delft, 1965.

4. Van Dyke, P., "Stresses about a Circular Hole in a Cylindrical Shell," AIAA Journal, Vol. 3, No. 9, Sept. 1965, pp. 1733-1742.

5. Savin, G. N., Stress Distribution Around Holes, Naukova Dumka Press, Kiev, 1968; Translation, NASA TT F-607, 1970, pp. 846-869.

6. Tennyson, R. C., "The Effects of Unreinforced Circular Cutouts on the Buckling of Circular Cylindrical Shells under Axial Compression," Journal of Engineering for Industry, Trans. of ASME, Vol. 90, No. 4, Nov. 1968, pp. 541-546.

7. Jenkins, W. C., "Buckling of Cylinders with Cutouts under Combined Loading," MDAC Paper WD 1390, McDonnell-Douglas Astronautics Co., Western Division, 1970.

8. Starnes, J. H., Jr., "The Effect of a Circular Hole on the Buckling of Cylindrical Shells," Ph.D. Thesis, California Institute of Technology, 1970.

9. Starnes, J. H., Jr., "The Effects of Cutouts on the Buckling of Thin Shells," Thin-Shell Structures, edited by Fung, Y. C. and Sechler, E. E., Prentice Hall, 1974, pp. 289-304.

10. Brogan, F. A. and Almroth, B. O., "Buckling of Cylinders with Cutouts," AIAA Journal, Vol. 8, No. 2, Feb. 1970, pp. 236-240.

11. Almroth, B. O. and Holmes, A. M. C., "Buckling of Shells with Cutouts, Experiment and Analysis," Internal Journal of Solids and Structures, Vol. 8, No. 8, Aug. 1972, pp. 1057-1071.

REFERENCES (Cont'd)

12. Almroth, B. O., Brogan, F. A. and Marlowe, M. B., "Stability Analysis of Cylinders with Circular Cutouts," AIAA Journal, Vol. 11, No. 11, Nov. 1973, pp. 1582-1584.

13. Babcock, C. D., Jr., "Experiments in Shell Buckling," Thin-Shell Structures, edited by Fung, Y. C. and Sechler, E. E., pp. 345-362.

14. Sechler, E. E., Elasticity in Engineering, John Wiley and Sons, Inc., 1952, pp. 153-157.

TABLE I

RESULTS OF EXPERIMENTS ON SHELL 1

R = 4.0 inches, t = 0.01 inches

MAJOR AXIS VERTICAL

a	b	a/b	$\alpha = \sqrt{\frac{A}{\pi Rt}}$	$\mu = \frac{a+b}{2\sqrt{Rt}}$	P	P/P_{CL}
inches	inches				pounds	
0.0	0.0	——	0.0	0.0	150.0	0.544
0.100	0.100	1.00	0.500	0.500	150.0	0.544
0.200	0.100	2.00	0.707	0.750	150.0	0.544
0.200	0.133	1.50	0.817	0.835	150.0	0.544
0.200	0.200	1.00	1.000	1.000	150.0	0.544
0.300	0.200	1.50	1.225	1.250	137.5	0.499
0.400	0.200	2.00	1.414	1.500	122.5	0.444
0.400	0.400	1.00	2.000	2.000	103.6	0.376
0.600	0.400	1.50	2.449	2.500	96.3	0.350
0.800	0.400	2.00	2.828	3.000	91.3	0.331
0.800	0.800	1.00	4.000	4.000	90.0	0.327
1.200	0.800	1.50	4.899	5.000	86.3	0.313
1.600	0.800	2.00	5.657	6.000	86.3	0.313
1.600	1.600	1.00	8.000	8.000	62.5	0.227
2.400	1.600	1.50	9.798	10.000	58.8	0.213

TABLE 2

RESULTS OF EXPERIMENTS ON SHELL 2

R = 4.0 inches, t = 0.01 inches

MAJOR AXIS HORIZONTAL

a inches	b inches	a/b	$\alpha = \sqrt{\frac{A}{\pi Rt}}$	$\mu = \frac{a+b}{2\sqrt{Rt}}$	P pounds	P/P_{CL}
0.0	0.0	——	0.0	0.0	162.5	0.590
0.100	0.100	1.00	0.500	0.500	160.0	0.580
0.200	0.100	2.00	0.707	0.750	157.5	0.571
0.200	0.133	1.50	0.817	0.835	145.0	0.526
0.200	0.200	1.00	1.000	1.000	125.0	0.454
0.300	0.200	1.50	1.225	1.250	95.0	0.345
0.400	0.200	2.00	1.414	1.500	72.5*	0.263
					82.5	0.299
0.400	0.400	1.00	2.000	2.000	72.5*	0.263
					77.5	0.281
0.600	0.400	1.50	2.449	2.500	70.0*	0.254
					77.5	0.281
0.800	0.400	2.00	2.828	3.000	70.0*	0.254
					76.3	0.277
0.800	0.800	1.00	4.000	4.000	72.5*	0.263
					77.5	0.281
1.200	0.800	1.50	4.899	5.000	67.5*	0.245
					70.0	0.254

---

*Local buckling - all other values are general collapse.

TABLE 2 (Cont'd)

RESULTS OF EXPERIMENTS ON SHELL 2

R = 4.0 inches, t = 0.01 inches

MAJOR AXIS HORIZONTAL

a inches	b inches	a/b	$\alpha = \sqrt{\frac{A}{\pi Rt}}$	$\mu = \frac{a+b}{2\sqrt{Rt}}$	P pounds	P/P_{CL}
1.600	0.800	2.00	5.657	6.000	60.0*	0.218
					62.5	0.227
2.400	1.600	1.50	9.798	10.000	40.0*	0.145
					47.5	0.172

---

*Local buckling

TABLE 3

RESULTS OF EXPERIMENTS ON SHELL 3

R = 4.0 inches, t = 0.01 inches

CIRCULAR CUTOUTS

a	a/R	A	$\alpha = \sqrt{\frac{A}{\pi Rt}}$	P	P/P_{CL}
inches		square inches		pounds	
0.0	0.0	0.0	0.0	190.0	0.689
0.100	0.0250	0.0314	0.500	185.0	0.671
0.133	0.0333	0.0256	0.667	182.5	0.662
0.141	0.0353	0.0628	0.707	182.5	0.662
0.163	0.0408	0.0838	0.817	180.0	0.653
0.200	0.0500	0.1257	1.000	155.0	0.562
0.245	0.0613	0.1885	1.225	132.5	0.481
0.283	0.0708	0.2513	1.414	120.0	0.435
0.400	0.10	0.5027	2.000	102.5	0.372
0.490	0.1215	0.7540	2.449	96.3	0.349
0.566	0.1915	1.0053	2.828	91.3	0.331
0.800	0.20	2.0106	4.000	85.0	0.308
0.980	0.2450	3.0159	4.899	83.8	0.304
1.131	0.2828	4.0212	5.657	78.8	0.286
1.600	0.40	8.0425	8.000	62.5	0.227

TABLE 4

RESULTS OF EXPERIMENTS ON SHELL 5

R = 4.0 inches, t = 0.01 inches

MAJOR AXIS HORIZONTAL

a	b	a/b	$\alpha = \sqrt{\frac{A}{\pi Rt}}$	$\mu = \frac{a+b}{2\sqrt{Rt}}$	P	P/P_{CL}
inches	inches				pounds	
0.0	0.0	———	0.0	0.0	195.0	0.707
0.100	0.100	1.00	0.500	0.500	196.25	0.712
0.200	0.100	2.00	0.707	0.750	185.0	0.671
0.200	0.133	1.50	0.817	0.835	170.0	0.617
0.200	0.200	1.00	1.000	1.000	150.0	0.544
0.300	0.200	1.50	1.225	1.250	127.5	0.463
0.400	0.200	2.00	1.414	1.500	113.75	0.413
0.400	0.400	1.00	2.000	2.000	93.75*	0.340
					100.00	0.363
0.600	0.400	1.50	2.449	2.500	90.00*	0.327
					96.75	0.351
0.800	0.400	2.00	2.828	3.000	87.50*	0.317
					90.00	0.327
0.800	0.800	1.00	4.000	4.000	85.0*	0.308
					88.75	0.322
1.200	0.800	1.50	4.899	5.000	77.5*	0.281
					80.5	0.292
1.600	0.800	2.00	5.657	6.000	68.75*	0.249
					71.25	0.259

---

*Local buckling

TABLE 4 (Cont'd)

RESULTS OF EXPERIMENTS ON SHELL 5

R = 4.0 inches, t = 0.01 inches

MAJOR AXIS HORIZONTAL

a	b	a/b	$\alpha = \sqrt{\frac{A}{\pi Rt}}$	$\mu = \frac{a+b}{2\sqrt{Rt}}$	P	P/P_{CL}
inches	inches				pounds	
1.600	1.600	1.00	8.000	8.000	62.5*	0.227
					65.0	0.236
2.400	1.600	1.50	9.798	10.000	51.25	0.186

---

*Local buckling

TABLE 5

RESULTS OF EXPERIMENTS ON SHELL 6

R = 4.0 inches, t = 0.01 inches

MAJOR AXIS ALTERNATELY VERTICAL AND HORIZONTAL

a	b	a/b	$\alpha = \sqrt{\frac{A}{\pi Rt}}$	$\mu = \frac{a+b}{2\sqrt{Rt}}$	P	P/P_{CL}
inches	inches				pounds	
0.0	0.0	——	0.0	0.0	200.0	0.726
0.100	0.100	1.00	0.500	0.500	198.75	0.721
0.200[V]	0.100	2.00	0.707	0.750	187.5	0.680
0.200[V]	0.133	1.50	0.817	0.835	171.25	0.621
0.200	0.200	1.00	1.000	1.000	155.0	0.562
0.300[H]	0.200	1.50	1.225	1.250	137.5	0.499
0.400[H]	0.200	2.00	1.414	1.500	118.75	0.431
0.400	0.400	1.00	2.000	2.000	96.25*	0.349
					105.0	0.381
0.600[V]	0.400	1.50	2.449	2.500	93.75*	0.340
					102.5	0.372
0.800[V]	0.400	2.00	2.828	3.000	82.5*	0.299
					91.25	0.331
0.800	0.800	1.00	4.000	4.000	76.25*	0.277
					80.0	0.290
1.200[H]	0.800	1.50	4.899	5.000	67.5*	0.245
					77.5	0.281

V Major axis vertical
H Major axis horizontal
* Local buckling

TABLE 5 (Cont'd)

RESULTS OF EXPERIMENTS ON SHELL 6

R = 4.0 inches, t = 0.01 inches

MAJOR AXIS ALTERNATELY VERTICAL AND HORIZONTAL

a	b	a/b	$\alpha = \sqrt{\frac{A}{\pi Rt}}$	$\mu = \frac{a+b}{2\sqrt{Rt}}$	P	P/P_{CL}
inches	inches				pounds	
1.600[H]	0.800	2.00	5.657	6.000	60.0*	0.218
					70.0	0.254
2.400[V]	1.600	1.50	9.798	10.000	52.5*	0.191
					55.5	0.201

V Major axis vertical
H Major axis horizontal
* Local buckling

TABLE 6

RESULTS OF EXPERIMENTS ON SHELL 9

R = 4.0 inches, t = 0.01 inches

SQUARE AND RECTANGULAR CUTOUTS

a inches	b inches	a/b	$\alpha = \sqrt{\frac{A}{\pi Rt}}$	$\mu = \frac{a+b}{2\sqrt{Rt}}$	P pounds	P/P_{CL}
0.0	0.0	——	0.0	0.0	143.75	0.522
0.100	0.100	1.00	0.564	0.500	143.0	0.519
0.200	0.100	2.00	0.798	0.750	136.25	0.494
0.200	0.133	1.50	0.921	0.835	130.0	0.472
0.200	0.200	1.00	1.128	1.000	112.5	0.408
0.300	0.200	1.50	1.382	1.250	92.5*	0.336
					95.0	0.345
0.400	0.200	2.00	1.596	1.50	82.5*	0.299
					91.25	0.331
0.400	0.400	1.00	2.257	2.00	78.75*	0.286
					86.25	0.313
0.600	0.400	1.50	2.764	2.50	76.25*	0.277
					83.0	0.301
0.800	0.400	2.00	3.192	3.00	75.0*	0.272
					81.25	0.295
0.800	0.800	1.00	4.514	4.00	70.0*	0.254
					78.85	0.286

---

*Local buckling

TABLE 6 (Cont'd)

RESULTS OF EXPERIMENTS ON SHELL 9

R = 4.0 inches, t = 0.01 inches

SQUARE AND RECTANGULAR CUTOUTS

a	b	a/b	$\alpha = \sqrt{\frac{A}{\pi Rt}}$	$\mu = \frac{a+b}{2\sqrt{Rt}}$	P	P/P_{CL}
inches	inches				pounds	
1.200	0.800	1.50	5.528	5.00	67.5*	0.245
					73.75	0.268
1.600	0.800	2.00	6.383	6.00	62.25*	0.227
					66.25	0.240
1.600	1.600	1.00	9.027	8.00	51.25*	0.186
					52.00	0.189

---

*Local buckling

TABLE 7

RESULTS OF EXPERIMENTS ON SHELL 5
UNDER ECCENTRIC AXIAL LOADS

R = 4.0 inches, t = 0.01 inches
y = Load Offset from ℄ - Perpendicular to
Axis Joining the Cutouts

a	b	$\alpha = \sqrt{\frac{A}{\pi Rt}}$	y	P	P/P_{CL}
inches	inches		inches	pounds	
0.0	0.0	0.0	-0.375	175.0	0.635
			-0.25	176.25	0.639
			-0.125	187.5	0.680
			0.0	195.0	0.707
			0.125	201.25	0.730
			0.25	187.5	0.680
			0.375	175.0	0.635
0.100	0.100	0.50	-0.375	173.75	0.630
			-0.25	180.0	0.653
			-0.125	190.0	0.689
			0.0	196.25	0.712
			0.125	197.5	0.717
			0.25	180.0	0.653
			0.375	175.0	0.635
0.200	0.100	0.707	-0.25	180.0	0.653
			-0.125	182.5	0.662
			0.0	185.0	0.671
			0.125	182.5	0.662
			0.25	180.0	0.653

TABLE 7 (Cont'd)

RESULTS OF EXPERIMENTS ON SHELL 5
UNDER ECCENTRIC AXIAL LOADS

R = 4.0 inches, t = 0.01 inches
y = Load Offset from ℄ - Perpendicular to
Axis Joining the Cutouts

a	b	$\alpha = \sqrt{\frac{A}{\pi Rt}}$	y	P	P/P_{CL}
inches	inches		inches	pounds	
0.200	0.133	0.817	-0.25	165.0	0.599
			-0.125	167.5	0.608
			0.0	170.0	0.617
			0.125	170.0	0.617
			0.25	168.75	0.612
0.200	0.200	1.000	-0.25	145.0	0.526
			-0.125	147.5	0.535
			0.0	150.0	0.544
			0.125	147.5	0.535
			0.25	145.0	0.526
0.300	0.200	1.225	-0.25	122.5	0.444
			-0.125	127.5	0.463
			0.0	127.5	0.463
			0.125	127.5	0.463
			0.25	127.5	0.463

TABLE 7 (Cont'd)

RESULTS OF EXPERIMENTS ON SHELL 5
UNDER ECCENTRIC AXIAL LOADS

R = 4.0 inches, t = 0.01 inches
y = Load Offset from $\mathbb{C}$ - Perpendicular to
Axis Joining the Cutouts

a	b	$\alpha = \sqrt{\frac{A}{\pi Rt}}$	y	P	P/P_{CL}
inches	inches		inches	pounds	
0.400	0.200	1.414	-0.25	113.75	0.413
			-0.125	112.5	0.408
			0.0	113.75	0.413
			0.125	113.25	0.411
			0.25	112.5	0.408
0.400	0.400	2.00	-0.25	100.0	0.363
			-0.125	100.0	0.363
			0.0	100.0	0.363
			0.125	97.5	0.354
			0.25	97.5	0.354
0.600	0.400	2.449	-0.25	92.5	0.336
			-0.125	96.25	0.349
			0.0	96.75	0.351
			0.125	96.75	0.351
			0.25	93.75	0.340

TABLE 7 (Cont'd)

RESULTS OF EXPERIMENTS ON SHELL 5
UNDER ECCENTRIC AXIAL LOADS

R = 4.0 inches, t = 0.01 inches
y = Load Offset from $\mathbb{C}$ - Perpendicular to
Axis Joining the Cutouts

a	b	$\alpha = \sqrt{\frac{A}{\pi Rt}}$	y	P	P/P_{CL}
inches	inches		inches	pounds	
0.800	0.400	2.828	-0.25	90.0	0.327
			-0.125	92.5	0.336
			0.0	90.0	0.327
			0.125	92.75	0.337
			0.25	91.25	0.331
0.800	0.800	4.00	-0.25	88.75	0.322
			-0.125	88.75	0.322
			0.0	88.75	0.322
			0.125	90.0	0.327
			0.25	87.5	0.317
1.200	0.800	4.899	-0.25	78.75	0.286
			-0.125	80.0	0.290
			0.0	80.5	0.292
			0.125	78.75	0.286
			0.25	78.75	0.286

TABLE 7 (Cont'd)

RESULTS OF EXPERIMENTS ON SHELL 5
UNDER ECCENTRIC AXIAL LOADS

R = 4.0 inches, t = 0.01 inches
y = Load Offset from $\mathbb{C}$ - Perpendicular to
Axis Joining the Cutouts

a	b	$\alpha = \sqrt{\frac{A}{\pi Rt}}$	y	P	P/P_{CL}
inches	inches		inches	pounds	
1.600	0.800	5.657	-0.25	70.0	0.254
			-0.125	73.75	0.268
			0.0	71.25	0.259
			0.125	72.5	0.263
			0.25	72.5	0.263
			0.375	72.5	0.263
			0.50	70.0	0.254
1.600	1.600	8.00	-0.25	65.0	0.236
			-0.125	65.0	0.236
			0.0	65.0	0.236
			0.125	63.75	0.231
			0.25	65.0	0.236
2.400	1.600	9.798	-0.25	50.0	0.181
			-0.125	50.25	0.182
			0.0	51.25	0.186
			0.125	53.0	0.192
			0.25	51.25	0.186

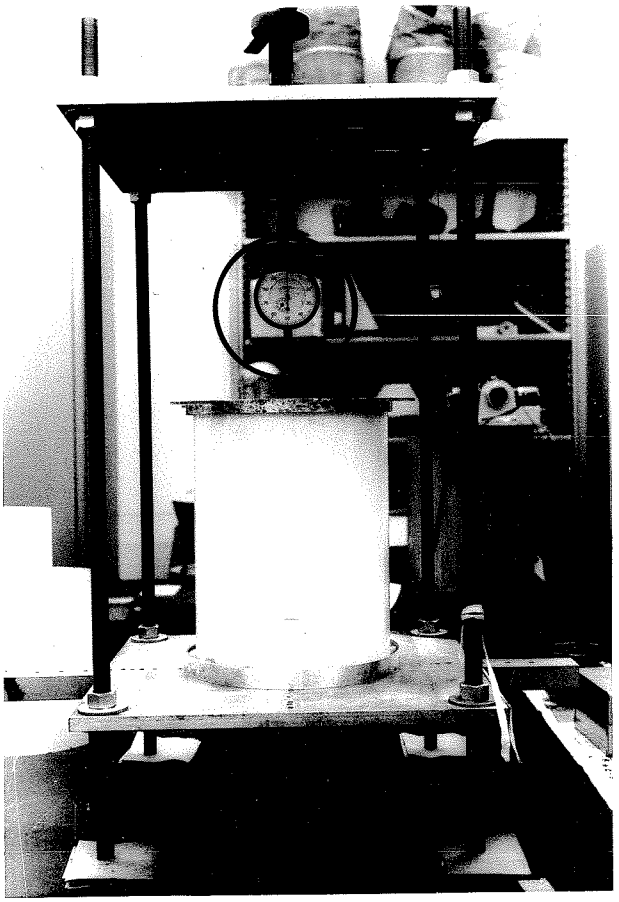

FIG.1 TEST APPARATUS

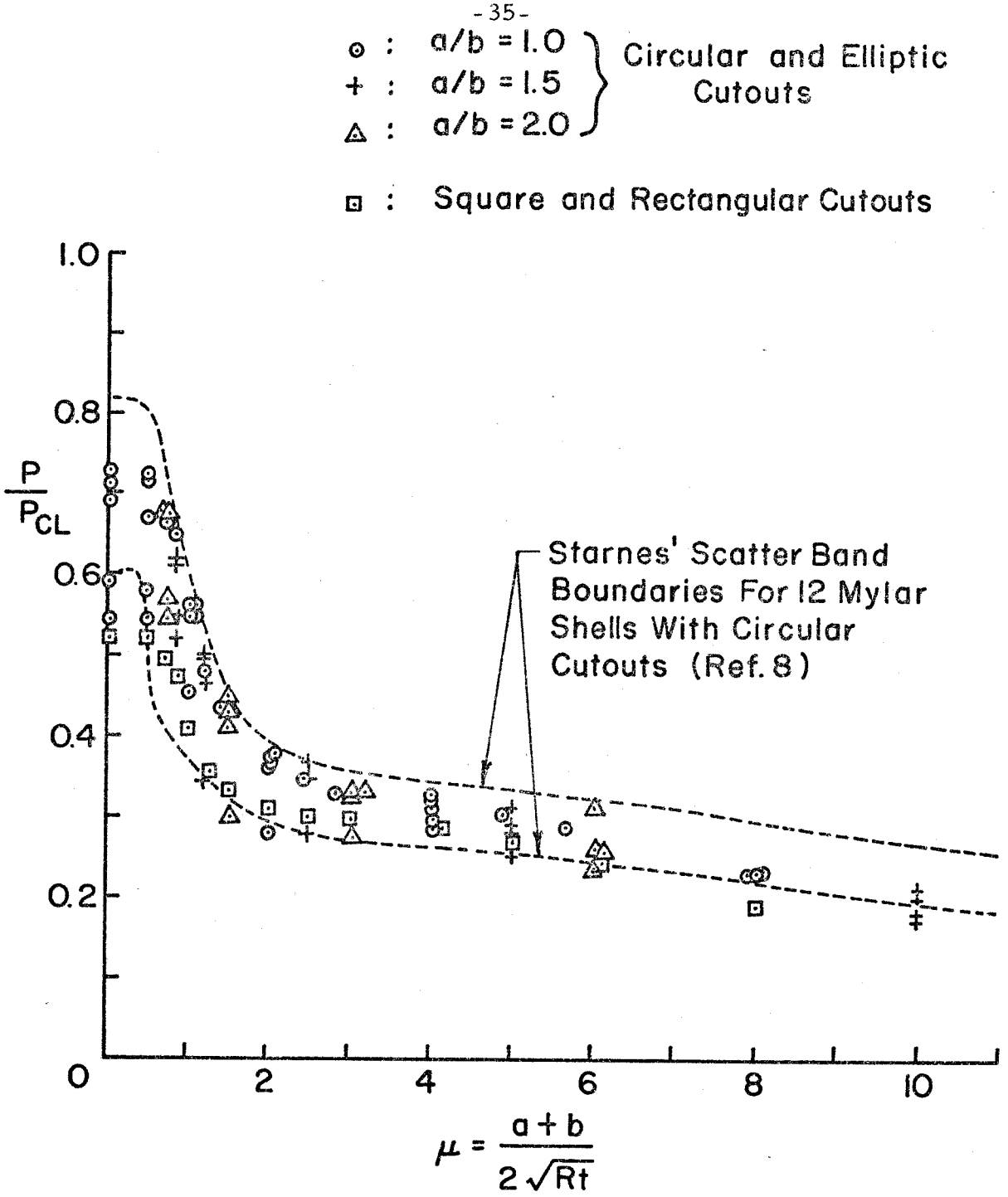

FIG. 2 SUMMARY OF EXPERIMENTAL RESULTS. THE EFFECTS OF CUTOUTS ON THE BUCKLING OF CIRCULAR CYLINDERS.

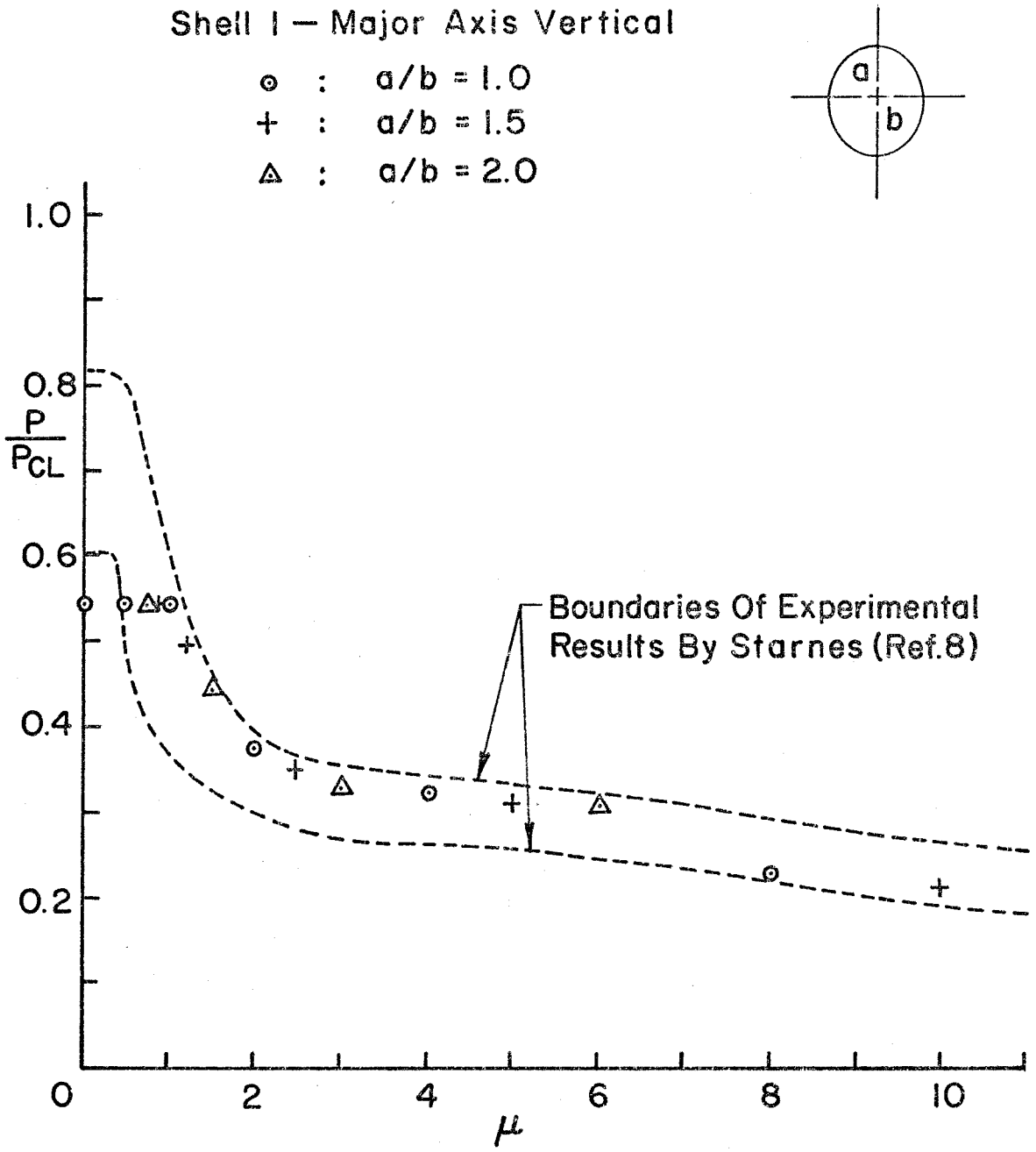

FIG. 3 BUCKLING LOADS OF SHELL I

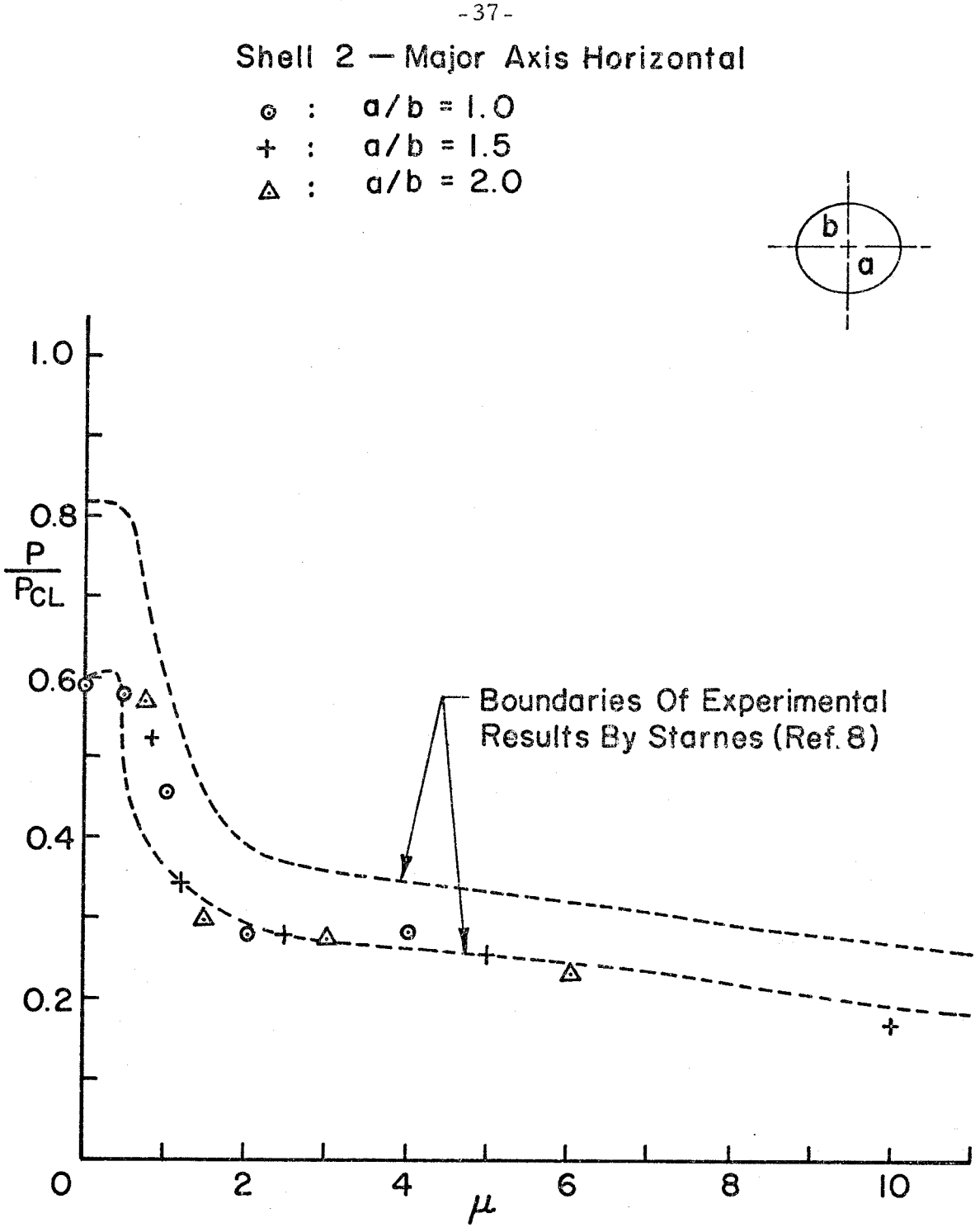

FIG. 4 BUCKLING LOADS OF SHELL 2

Shell 3 - Circular Cutouts

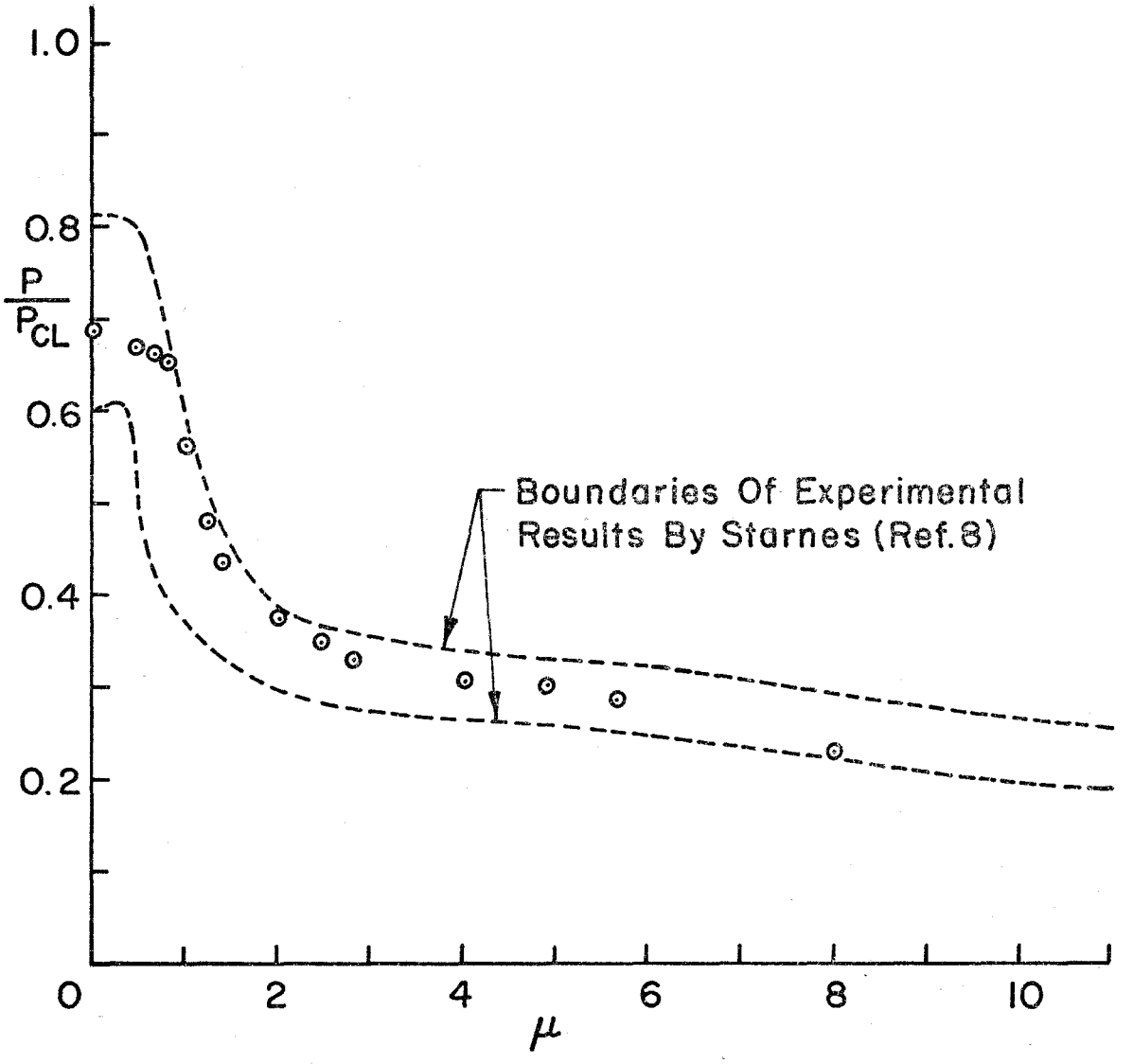

FIG. 5 BUCKLING LOADS OF SHELL 3

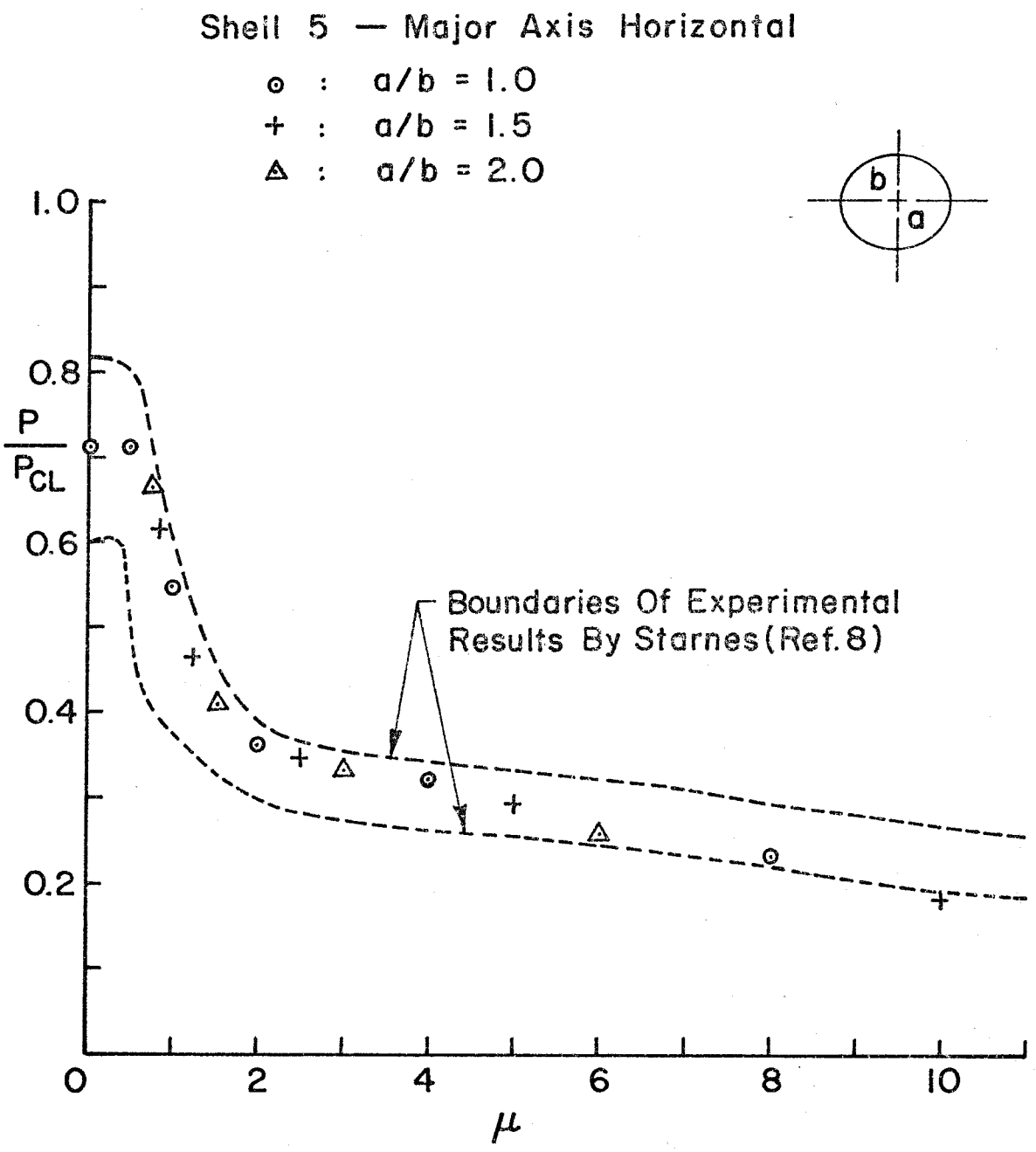

FIG. 6 BUCKLING LOADS OF SHELL 5

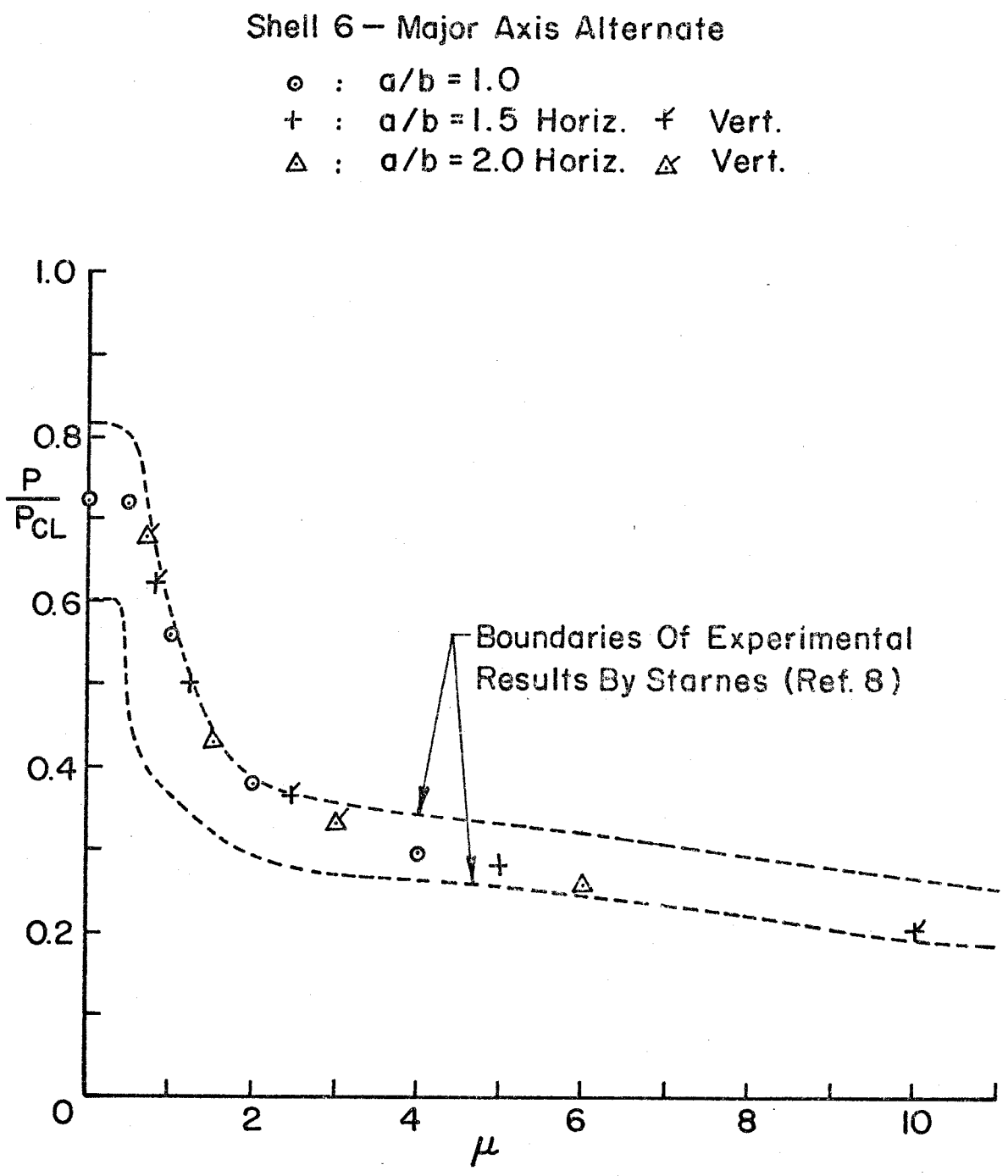

FIG. 7 BUCKLING LOADS OF SHELL 6

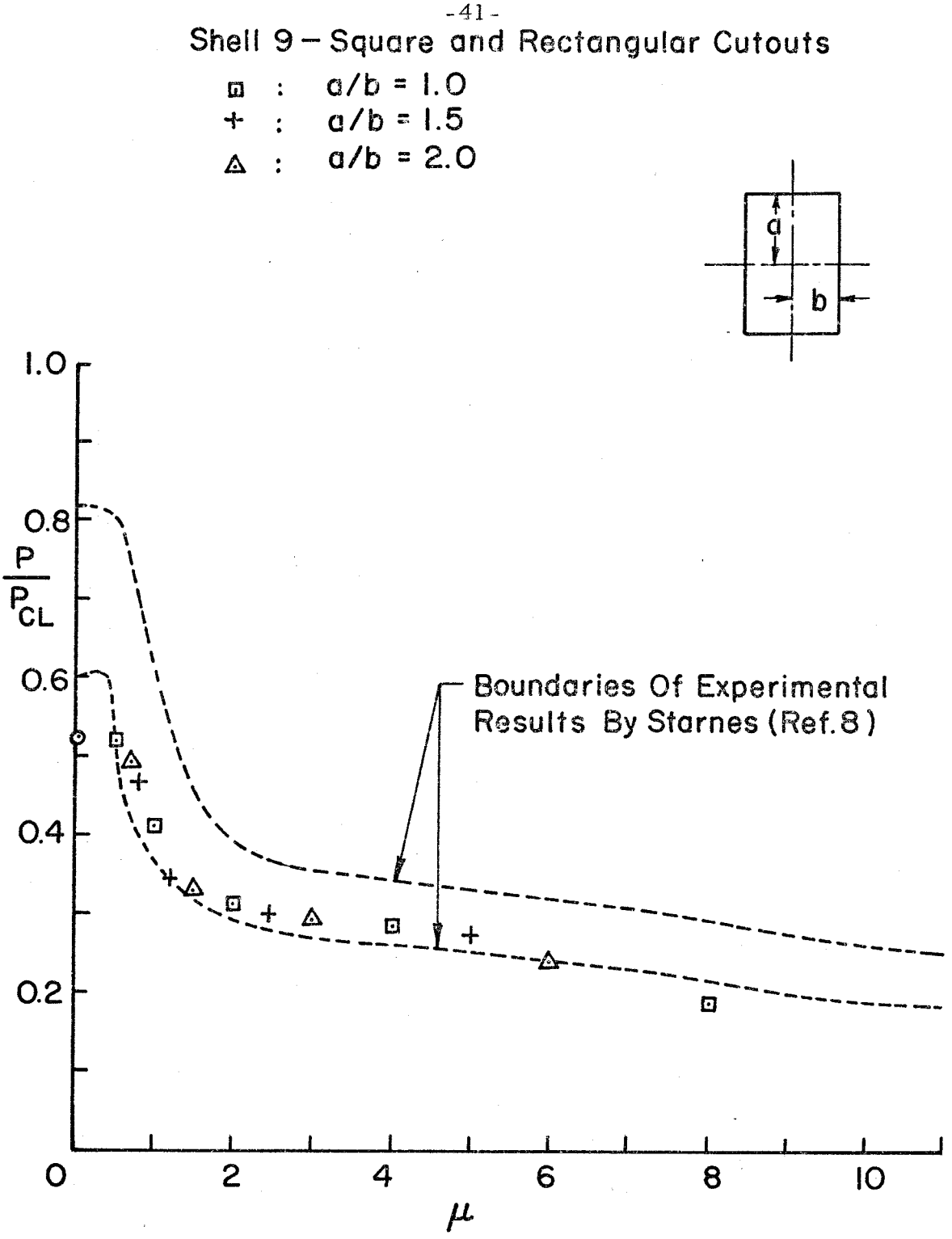

FIG. 8 BUCKLING LOADS OF SHELL 9

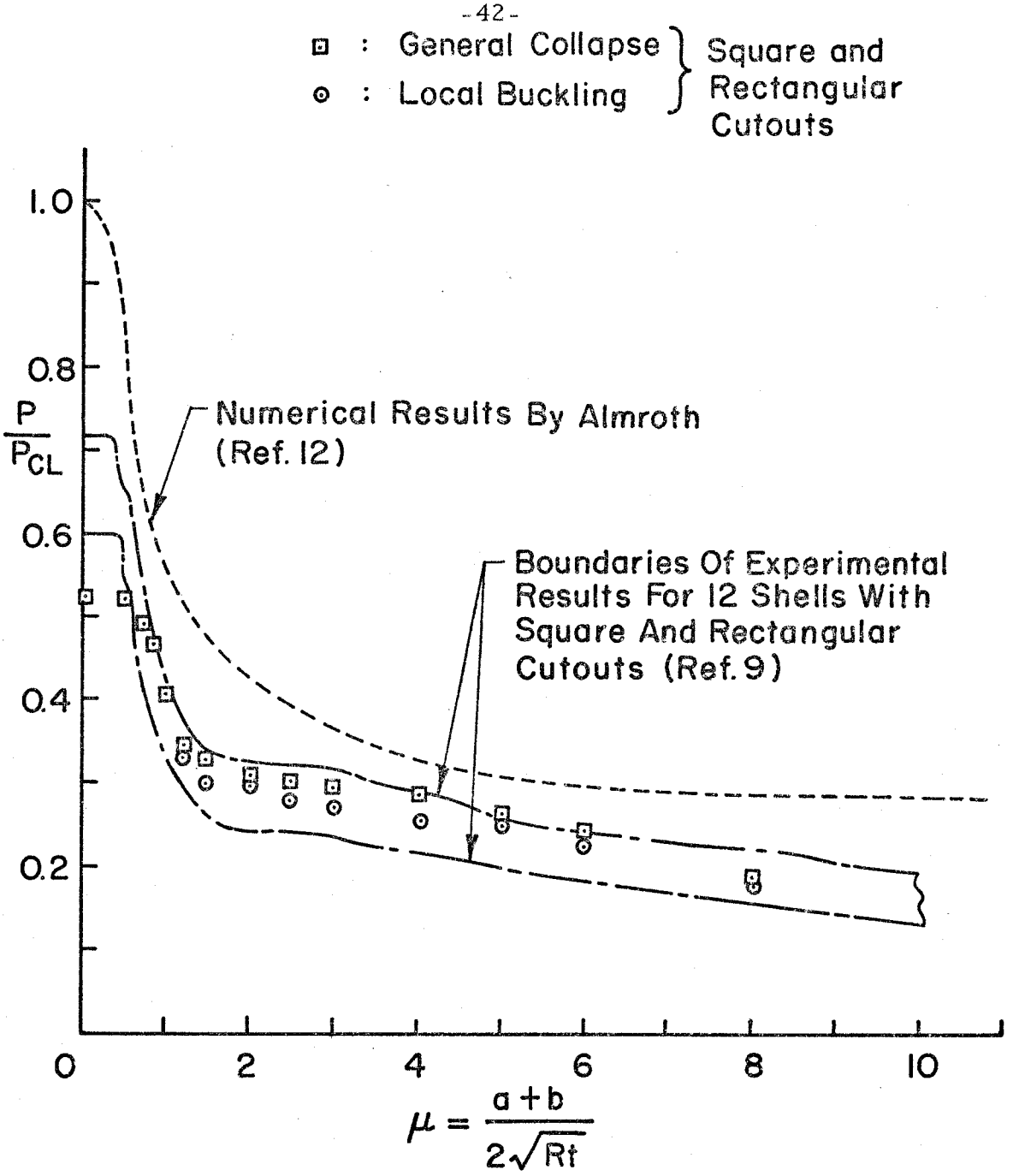

FIG. 9 THE EFFECTS OF SQUARE AND RECTANGULAR CUTOUTS ON THE BUCKLING OF CIRCULAR CYLINDERS

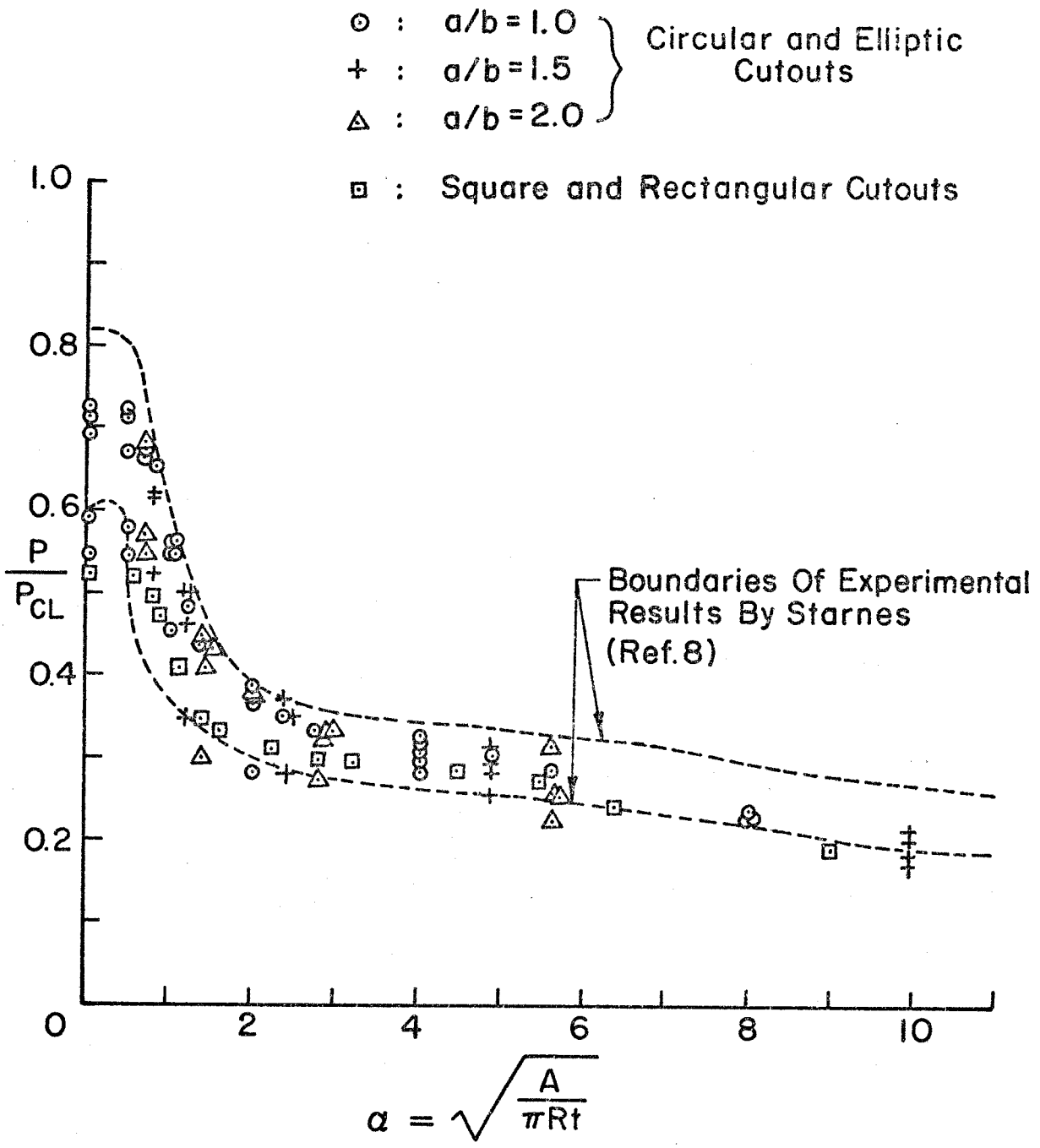

FIG. 10 SUMMARY OF EXPERIMENTAL RESULTS. THE EFFECTS OF CUTOUTS ON THE BUCKLING OF CIRCULAR CYLINDERS.

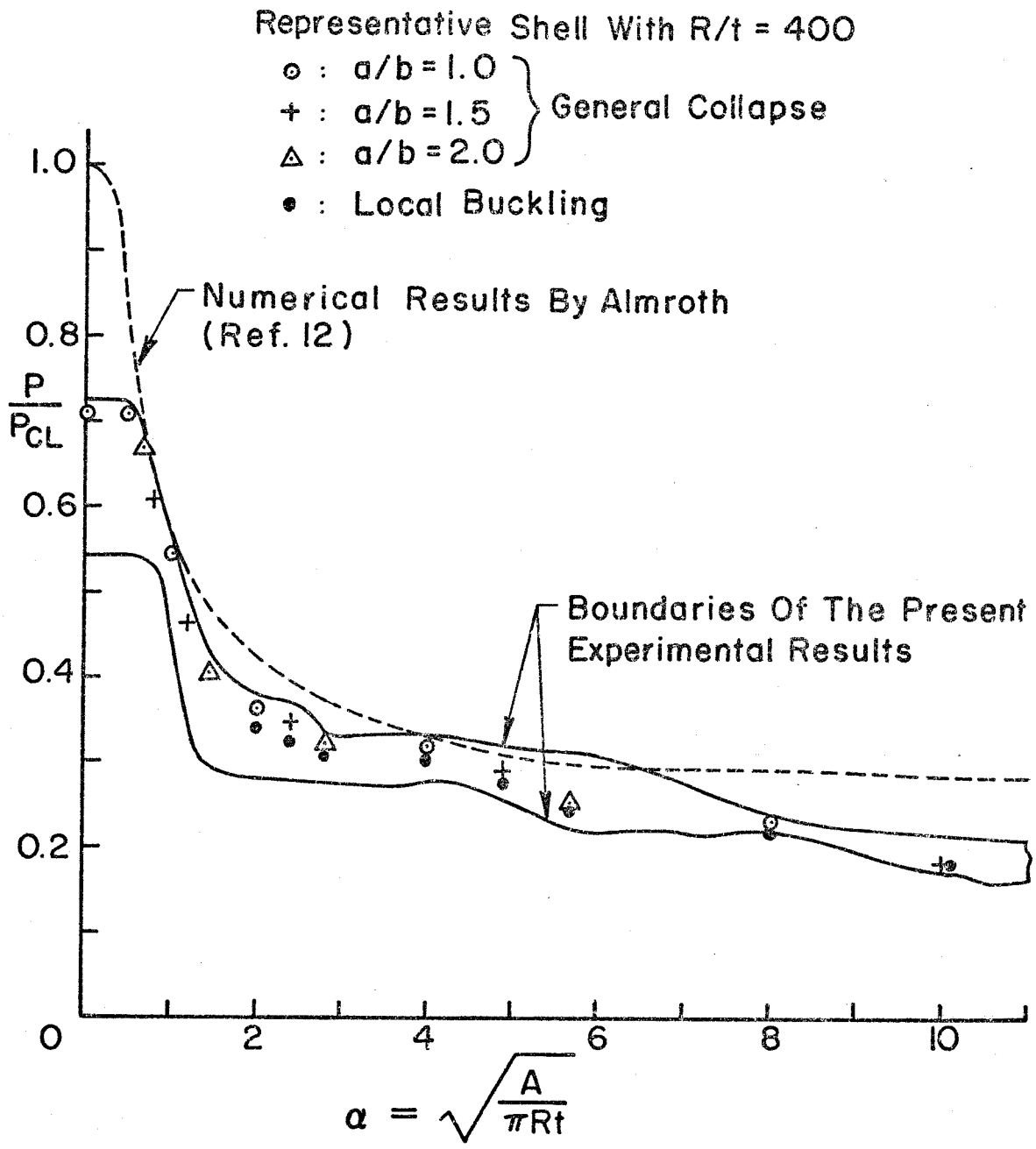

FIG. 11 THE EFFECTS OF ELLIPTIC CUTOUTS ON THE BUCKLING OF CIRCULAR CYLINDERS

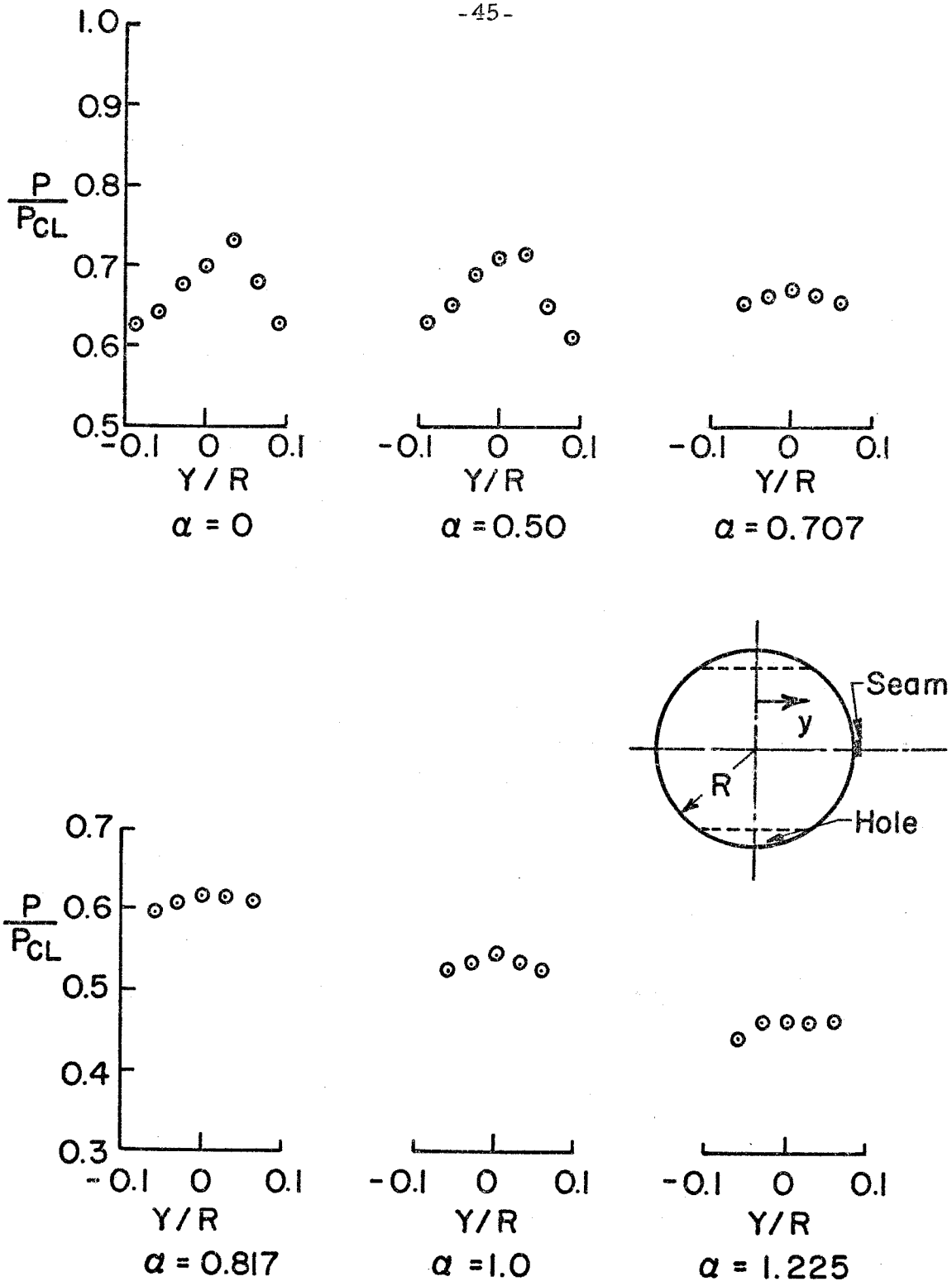

FIG.12 EFFECT OF LOAD LOCATION ON THE BUCKLING LOADS OF SHELL 5

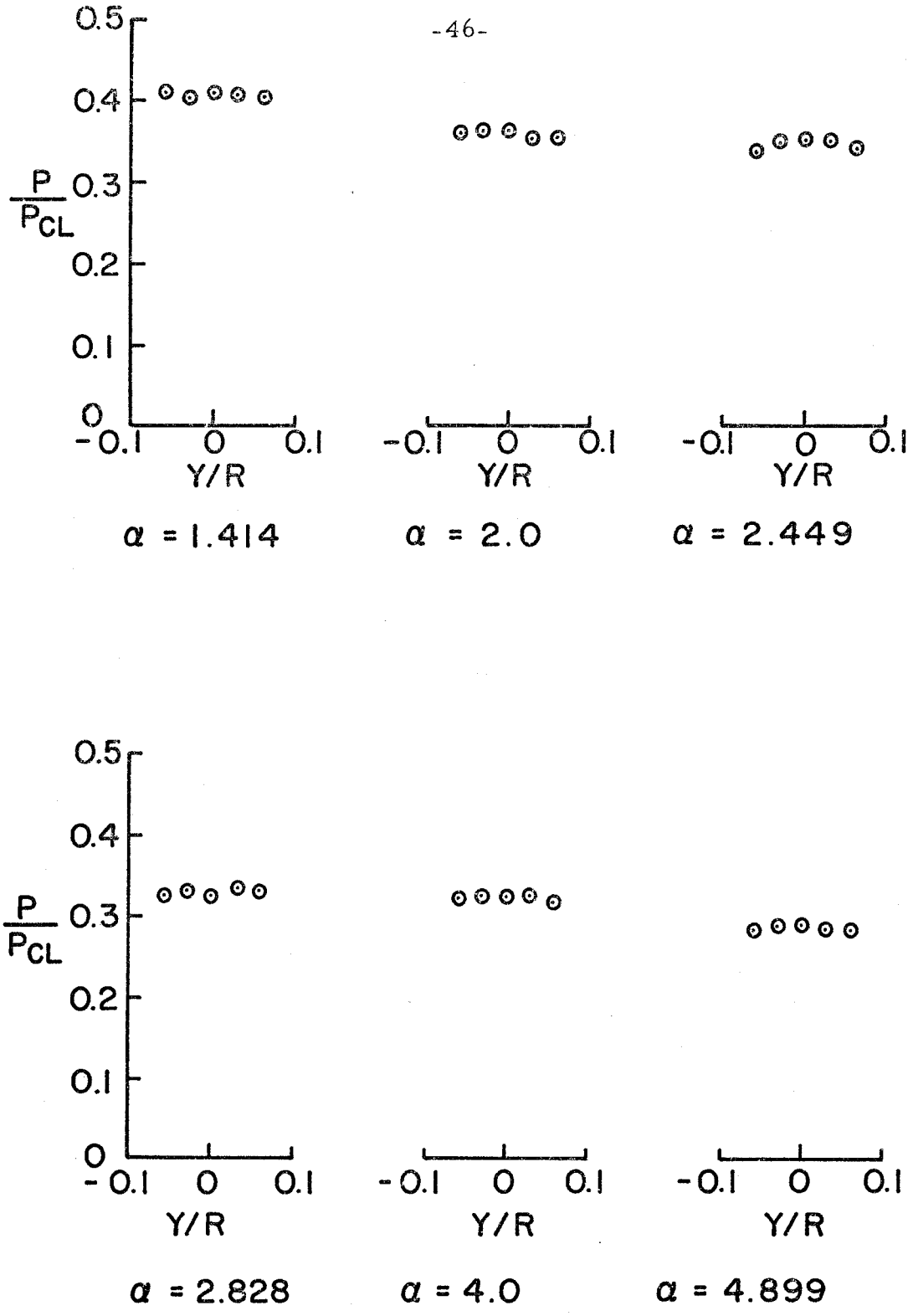

FIG. 12 (cont'd.) EFFECT OF LOAD LOCATION ON THE BUCKLING LOADS OF SHELL 5

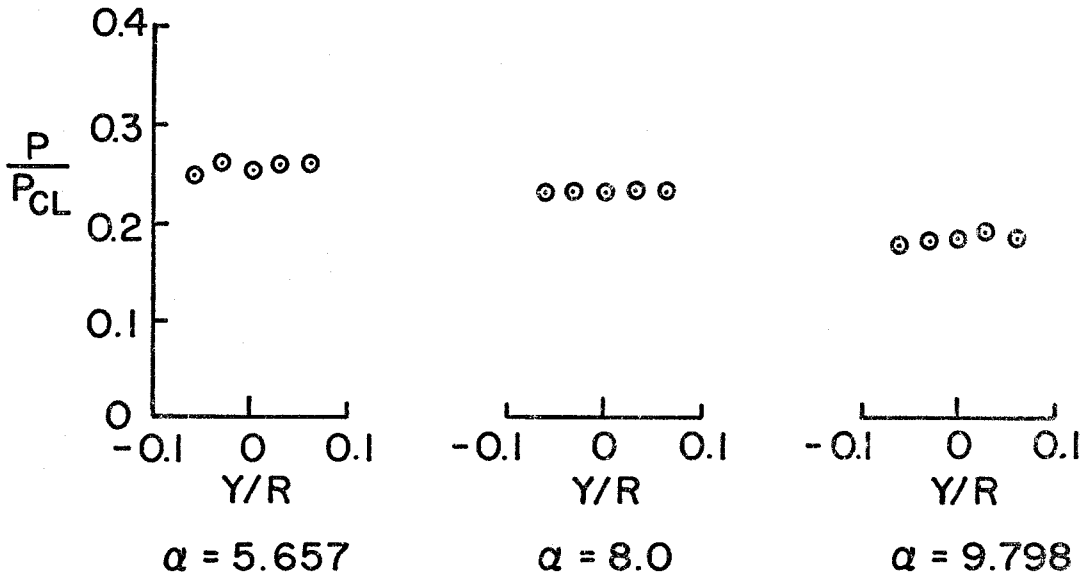

FIG. 12 (cont'd) EFFECT OF LOAD LOCATION ON THE BUCKLING LOADS OF SHELL 5

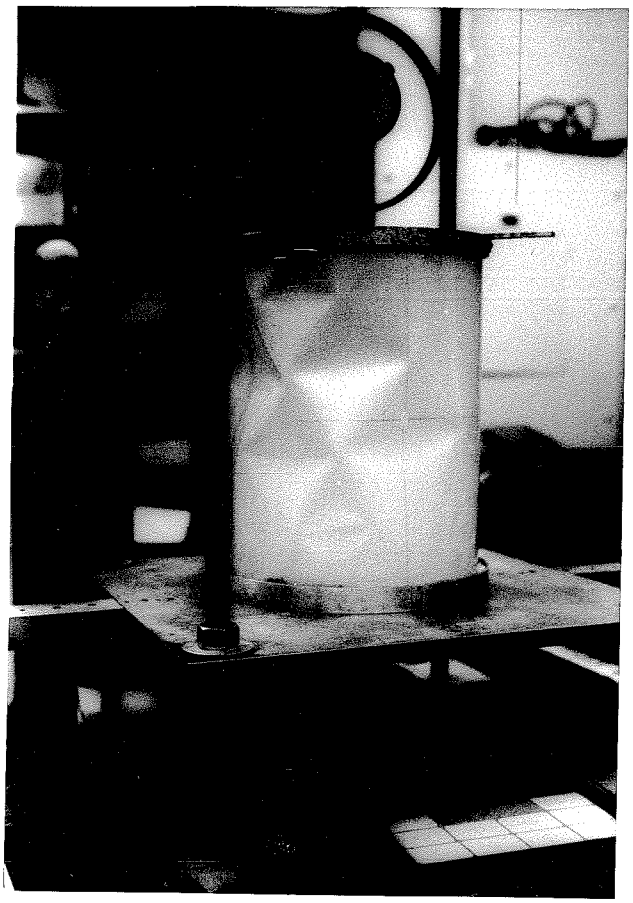

FIG.13 BUCKLING MODE FOR $\alpha < 2$

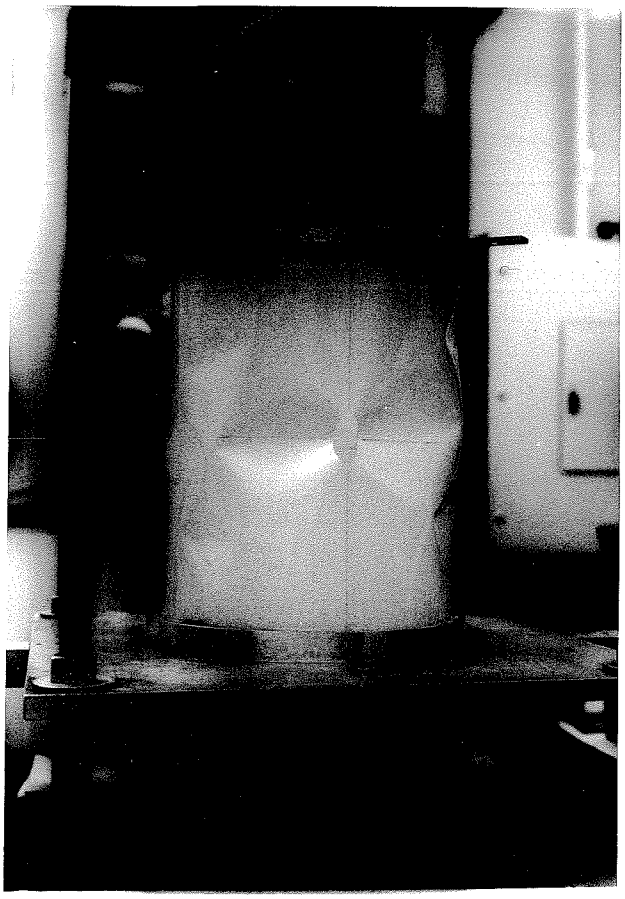

FIG.14 BUCKLING MODE FOR $\alpha \geqslant 2$

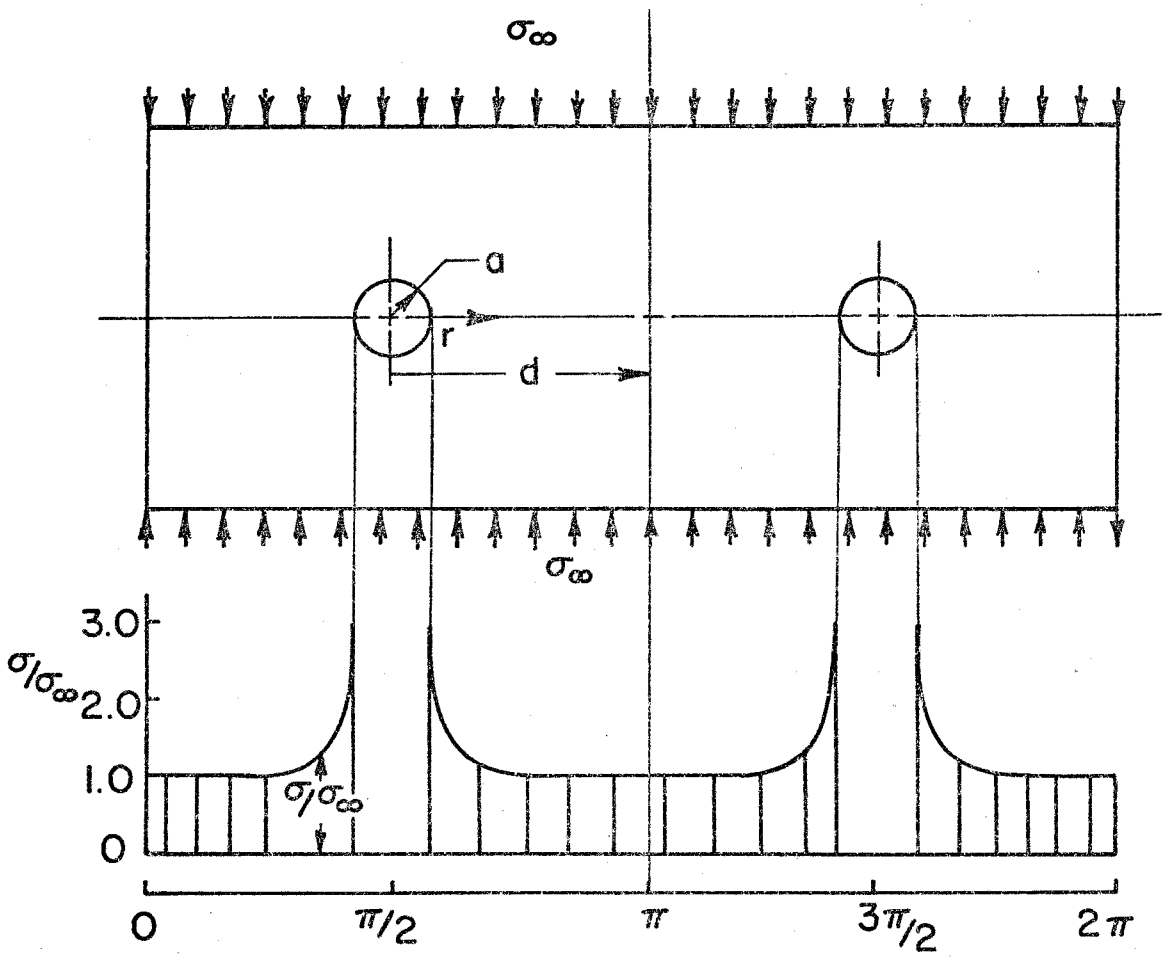

FIG. 15 THE DEVELOPED CYLINDER WITH TWO CUTOUTS

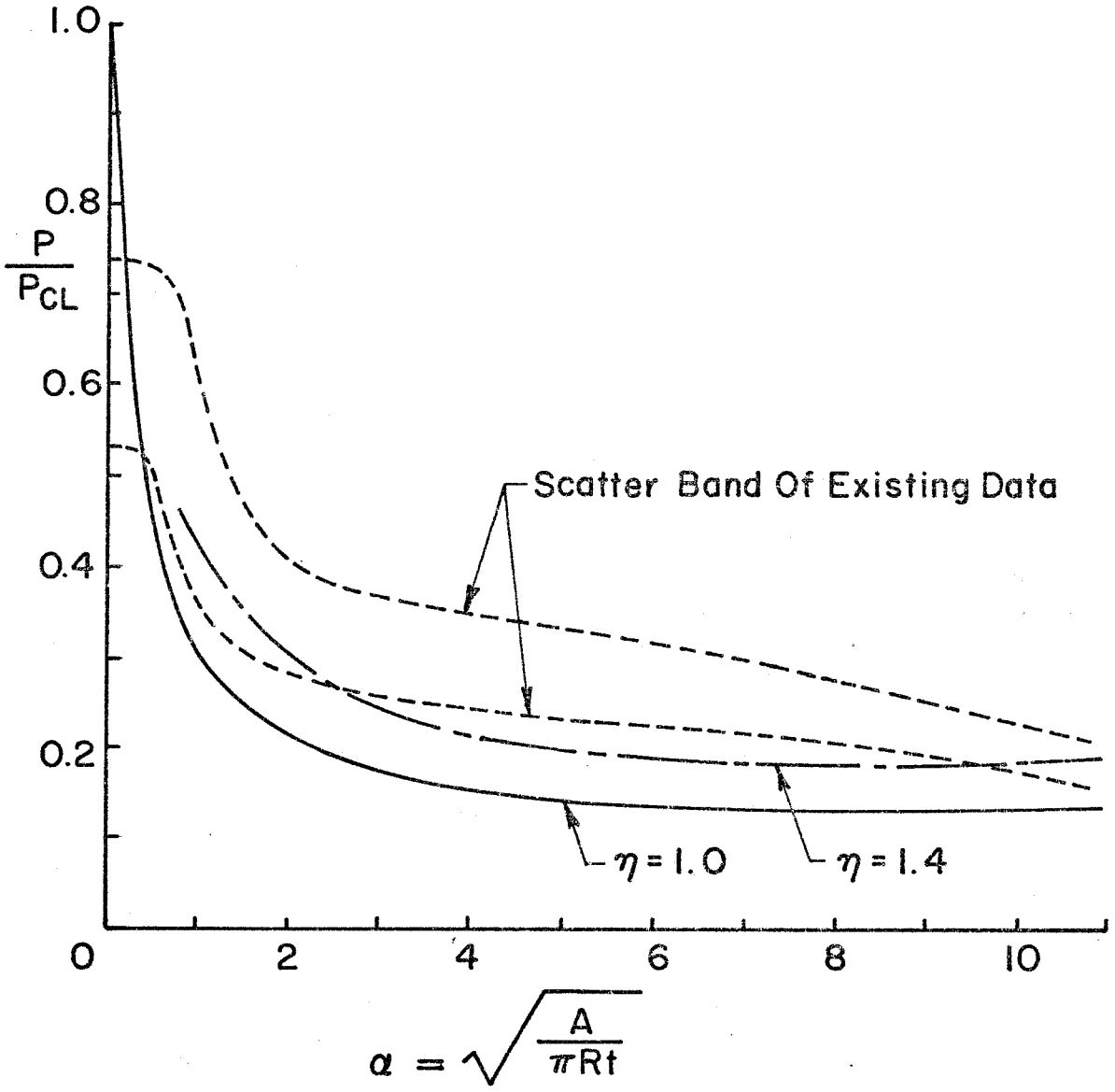

FIG. 16 SUMMARY OF THE BUCKLING LOADS AND ANALYSIS

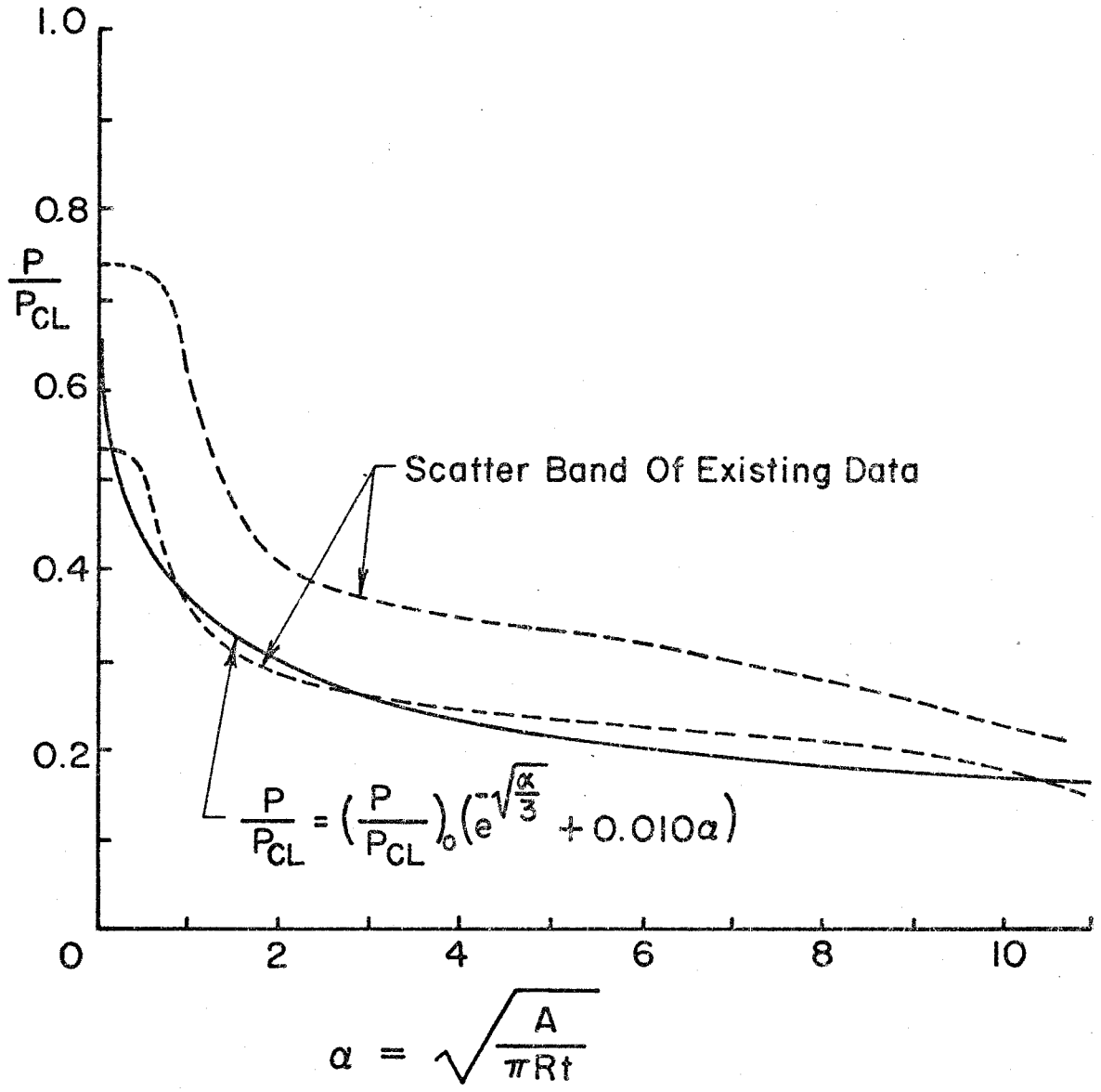

FIG. 17 SUMMARY OF THE BUCKLING LOADS AND AN EMPIRICAL FORMULA